

Studies of the Swelling and Drying Kinetics of Thin Gelatin Gel Films by *in Situ* Interferometry

Chi Wu* and Chui-Ying Yan

Department of Chemistry, The Chinese University of Hong Kong, Shatin, N.T., Hong Kong, China

Received December 3, 1993; Revised Manuscript Received April 26, 1994*

ABSTRACT: Both the swelling and drying kinetics of thin gelatin gel films were studied by *in situ* interferometry. Both a novel interferometry sensor and a conventional interferometer were used. One of the advantages of using the *in situ* interferometers is that the experimental time required to reach final swelling equilibrium has been reduced from hours, or even days, to minutes. The basic principle of *in situ* interferometry is illustrated. Our swelling experimental data can be better fitted by the first-order kinetics than by the suggested second-order one in literatures. This apparent contradiction has been discussed in terms of the difference in the size of gelatin gel. The experimental data obtained in the drying process show that the film-drying rate increases with time, while according to the general gel-shrinking theory developed by Li and Tanaka the gel-shrinking rate should decrease with time. We have shown that the deviation might be attributed to the intrinsic difference between the drying and shrinking processes, i.e., one is in dry air and another is in solvent, and to the nature of gelatin gel. In addition, the ratio of the shear modulus over the longitudinal modulus and the cooperative diffusion coefficient were also estimated from the swelling experimental results.

Introduction

Both theoretical and experimental aspects of the equilibrium swelling and shrinking of semicrystalline (cross-linked) polymer networks or gels in liquids have been extensively studied.¹⁻⁵ However, few studies have dealt with the swelling, shrinking, and drying kinetics.⁶⁻¹⁰ In fact, the swelling, shrinking, and drying kinetics of physically or chemically cross-linked polymer gels (networks) are very important in numerous applications, such as in designing controlled-release devices for oral drugs, cosmetic ingredients, and agricultural pesticide, in producing storable foods/feeds, and in developing artificial muscles and organs.

Due to its nontoxic nature, gelatin has been widely and extensively used in food, photographic, and pharmaceutical industries as an important ingredient, such as for pulverulent formulations of vitamin A and carotenoids.^{11,12} Gelatin forms a class of proteinaceous substances derived from a naturally occurring parent protein, collagen, through some procedures which mostly involve the destruction of the secondary structure of the collagen. Gelatin is well-known for its property of forming elastic gels at room temperature in a relatively low concentration: a few percent of gelatin in water. During the gelation process, gelatin molecules renaturalize into a collagen-like structure: a triple-stranded helix. The studies of kinetics of swelling and drying of thin gelatin gel film are especially important when gelatin is used as a protective layer or coating on suspended colloid particles in pharmaceutical and food industries.

Besides the importance of the swelling and drying kinetics in various applications, the following two reasons prompted us to start the present work. First, the research results in the past have suggested that the swelling kinetics of gelatin gels can in general be expressed by^{9,13,14}

$$W = KW_{\infty}^2 t / (1 + KW_{\infty} t) \quad (1)$$

where W and W_{∞} are the swelling or solvent uptake at time t and at equilibrium, respectively. K is the rate

constant in the following differential equation:

$$dW/dt = K(W_{\infty} - W)^2 \quad (2)$$

Therefore, the experimental results suggest that the process of gelatin swelling follows a second-order kinetics. This second-order kinetics was explained by using the following assumption:⁹ The gelatin gel swelling rate is directly proportional to both $[(W_{\infty} - W)/W_{\infty}]$ and S , where $[(W_{\infty} - W)/W_{\infty}]$ is the relative or fractional amount of gelatin swelling capacity which is still available at time t and S is the internal specific boundary area which encloses those sites of the polymer network that have not yet interacted with water at time t but will be hydrated and swell in due course. S is further proportional to $[(W_{\infty} - W)/W_{\infty}]$. Thus, the swelling rate is proportional to the second order of $[(W_{\infty} - W)/W_{\infty}]$, i.e., $dW/dt \propto [(W_{\infty} - W)/W_{\infty}]^2$. But, this second-order kinetics apparently contradicts the existing theory of kinetics of swelling and shrinking of a cross-linked polymeric network.⁸ Second, most of the swelling and shrinking kinetic studies of gelatin gels in the past had used three-dimensional macroscopic size gelatin gels and the swelling and shrinking processes were monitored either by a conventional microscope or by a classic weighting method. It is well-known that for a macroscopic size gel, the swelling and shrinking of the portion near the gel surface may be different in comparison with the one in the center of the gel. This difference certainly complicates the kinetic studies. Therefore, the kinetic studies of very thin gel film by *in situ* interferometry will enable us to reduce this difference, but also provide a microscopic view of the kinetic process, so that a better understanding of both the swelling and drying kinetics can be acquired.

Theoretical Background

Kinetics of Swelling and Shrinking. Li and Tanaka predict that the kinetics of swelling and shrinking of a gel should follow the following equation:⁸

$$\frac{W_{\infty} - W}{W_{\infty}} = \sum_{n=1}^{\infty} B_n \exp(-t/\tau_n) \quad (3)$$

* Abstract published in *Advance ACS Abstracts*, June 1, 1994.

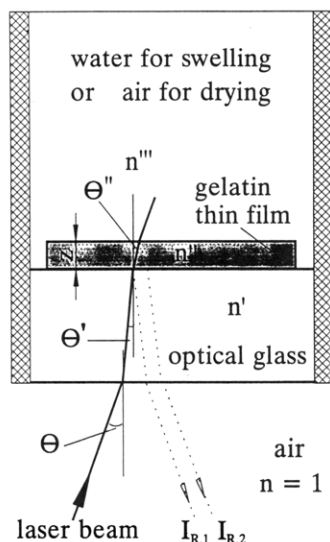


Figure 1. Schematic of a normal *in situ* interferometry setup, where a He-Ne laser is used as the laser light source and the two reflected light beams are interfered at a photodiode to produce a voltage signal (V). The angle θ has been enlarged for a clear view. In our real setup, θ is very close to 0, and so are both θ' and θ'' .

where B_n is a constant and related to the ratio of the shear osmotic modulus G and the longitudinal osmotic modulus M . In the limit of large t or if τ_1 is much larger than the rest of τ_n ,⁸ all high-order terms ($n \geq 2$) in eq 3 can be dropped so that the swelling and shrinking can be represented by the first-order kinetics

$$\ln\left(\frac{W_\infty - W}{W_\infty}\right) = \ln(B_1) - t/\tau_1 \quad (4)$$

or

$$dW/dt = (1/\tau_1)(W_\infty - W) \quad (5)$$

It should be noted from eq 3 that $\sum B_n = 1$. Therefore, B_1 should be less than 1 and the boundary conditions of eq 5 are between the limits 0, t for time and $W_\infty(1 - B_1)$, W for W . Further, B_1 is related to the ratio of the shear modulus G and the longitudinal osmotic modulus M by⁸

$$B_1 = \frac{2(3 - 4R)}{\alpha_1^2 - (4R - 1)(3 - 4R)} \quad (6)$$

where $R = G/M$, and τ_1 is related to the collective cooperative diffusion coefficient D_c of a gel disk at the surface by^{8,10}

$$D_c = \frac{3z_\infty^2}{\tau_1\alpha_1^2} \quad (7)$$

where z_∞ is the disk thickness in the final equilibrium state which can be experimentally determined and α_1 is a function of R , i.e.,

$$R = \frac{1}{4} \left[1 + \frac{\alpha_1 J_0(\alpha_1)}{J_1(\alpha_1)} \right] \quad (8)$$

Therefore, after finding the values of B_1 and τ_1 from the plot of $\ln[(W_\infty - W)/W_\infty]$ versus t at large t based on eq 4, we can obtain R and D_c by using a combination of eqs 6–8.

Interferometry. As schematically shown in Figure 1, when a laser light hits a thin film at an angle of θ' which

is smaller than the critical angle, it will be reflected twice by the two interfaces between the film and the surrounding mediums due to the refractive index difference. The two reflected light beams ($I_{R,1}$ and $I_{R,2}$) have an optical path difference of $2nz \cos(\theta'')$, where n and z are respectively the refractive index and the film thickness. The factor of 2 in $2nz \cos(\theta'')$ arises from dual passage of the laser beam through the film. Due to the interference between these two reflected light beams, the intensity (I) at the detector is a function of the film thickness (z),³ i.e.,

$$I = E_{R,1}^2 + E_{R,2}^2 + 2E_{R,1}E_{R,2} \cos\left[\frac{4\pi nz \cos(\theta'')}{\lambda_0}\right] \quad (9)$$

where $E_{R,1}$ and $E_{R,2}$ are respectively the electric fields of $I_{R,1}$ and $I_{R,2}$, i.e., $I_{R,1} = E_{R,1}^2$ and $I_{R,2} = E_{R,2}^2$; and λ_0 is the laser wavelength in vacuum. According to eq 9, if z is a function of time, I varies with z between the minimum $(E_{R,1} - E_{R,2})^2$ and the maximum $(E_{R,1} + E_{R,2})^2$. In this way, the change in the intensity I can be used to monitor the change in z .

Experimental Section

Sample Preparation. One laboratory-prepared gelatin (Pharma grade, 50100, A type from pig skin with a Bloom value 310) used in this experiment was courtesy of Dr. Wilfried Babel (Deutsche Gelatine-Fabriken Stoess AG, Eberbach). The weight- and number-average molecular weight are 2.92×10^5 and 1.27×10^5 g/mol, respectively. The gelatin gels were prepared by first dissolving a proper amount (10–20% in weight) of gelatin in a buffer solution (pH = 7.00) at 50 °C for at least 2 h to form a uniform gelatin solution, and then, the solution was cooled down to a certain temperature below the gelatin melting temperature to form gelatin gel. An estimate of 12% water in gelatin has been taken into account when we calculated the concentration. The thin gelatin gels with different thicknesses (15–90 μm) were made by using a high precision quadruple film applicator (Erichsen, Model 360).

In Situ Interferometry. A normal configuration of the *in situ* interferometer used in the present work is illustrated in Figure 1. The thin gel film was supported by a temperature-regulated optical glass plate. On the top of the film, there will be either dry air in the drying process or the buffer solution in the swelling process. A He-Ne laser (Uniphase 1135P, 10 mW, $\lambda_0 = 632.8$ nm) was used as a light source. In our present experimental setup,¹⁵ the angle θ is very close to 0, so are θ' and θ'' . Therefore, the term of $\cos(\theta'')$ in eq 9 can be dropped. The reflected lights ($I_{R,1}$ and $I_{R,2}$) were interfered at a photodiode (Hamamatsu S2386-18K) to produce a voltage signal which is proportional to the intensity I . The output signal was recorded through an analog-to-digital data acquisition system (an A-to-D board, National Instruments, AT-MIO16X plus an IBM/PC-AT486 personal computer).

This normal configuration can be integrated into a novel and miniature form as schematically shown in Figure 2, where a semiconductor laser (SONY, 1 mW, and $\lambda_0 = 730$ nm) and a photodiode detector (0.8 mm \times 0.4 mm) with a sensitivity of 0.4 $\mu\text{A}/\mu\text{W}$ were integrated to form a laser/detector hybrid. The laser chip and the detector chip are placed symmetrically about the optical axis of the lens. The distance between the laser chip and the detector chip is 1.0 ± 0.1 mm. The laser light is collimated by the lens (NA = 0.25; $f = 9$ mm). The collimated laser beam comes out from the lens at an angle of $\sim 2^\circ$ to the optical axis. The two reflected beams are focused by the same collimating lens to the photodiode detector. The outside dimension of the device is only 13 mm \times 22 mm. The working distance between the lens and the film can be as long as 50 mm. The laser and the detector can be operated by a laser driver together with an amplifier. This miniature interferometer sensor was mounted on a plate with x and y movements and two tilt freedoms. The alignment requires only a few minutes. The hybrid is commercially available as the detecting head in a normal compact disk (CD) player. It has been modified to suit our present application. The advantage of using this laser/detector hybrid

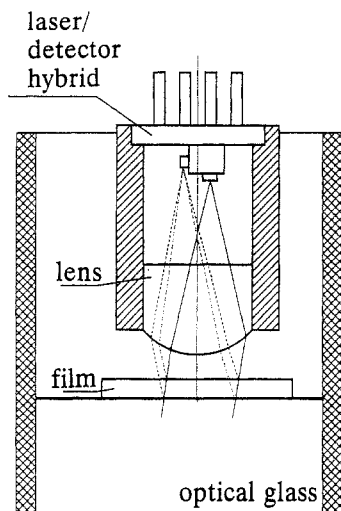


Figure 2. Schematic of a novel and miniature interferometry sensor, where a semiconductor laser and a photodiode detector were integrated to form a laser/detector hybrid (see text for details).

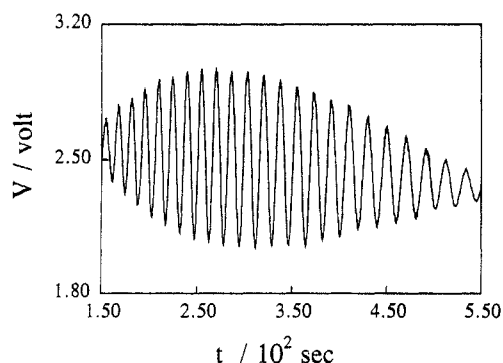


Figure 3. Part of typical voltage signal observed in the gel swelling process, where V is proportional to I in eq 9 (see text for details). The gel-swelling temperature is 29 °C, the initial gelatin concentration is 10%, and the initial film thickness is 60 μm .

is that it can be immersed into the buffer solution in swelling process so that the reflection from the interface between the buffer solution and the top air can be eliminated. It is important in practice to remove this kind of reflection since the interface between the buffer solution and air is moving and vibrating during the measurement.

Results and Discussion

Figure 3 shows one part of typical observed voltage signal in the swelling process, where V is proportional to I in eq 9. According to eq 9, the time between one maximum (minimum) to another maximum (minimum) corresponds to a thickness change of $\lambda_0/2n$. In both the swelling and drying process, the refractive index (n) of gelatin gel changes with time. The change of n as time can be separately determined by using a refractometer. After correcting n , we are able to transfer the signal profile in Figure 3 into the thickness change (Δz) versus time (t) which is shown in Figure 4. As expected, Δz increases as time and approaches to an equilibrium value (Δz_0) at $t = \infty$. It should be noted that the time corresponding to the first data point in Figure 4 is only a few seconds.

It should be noted that the study of thin gelatin gel film by *in situ* interferometry has three advantages in comparison with those conventional methods, such as microscope and weighting. First, the typical film size of $\sim 4 \text{ mm} \times 4 \text{ mm}$ is much larger than the typical film thickness ($\sim 0.060 \text{ mm}$), so that the film size in comparison with the

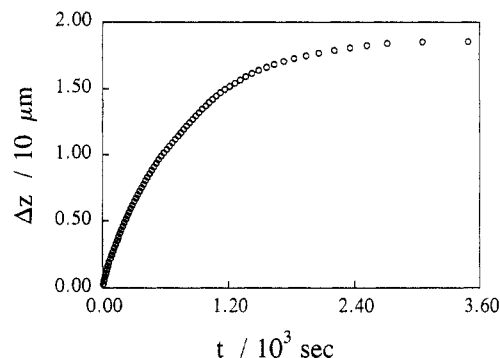


Figure 4. Film thickness change (Δz) versus time (t) during the swelling process, which is calculated on the basis of eq 3 from the signal profile in Figure 3.

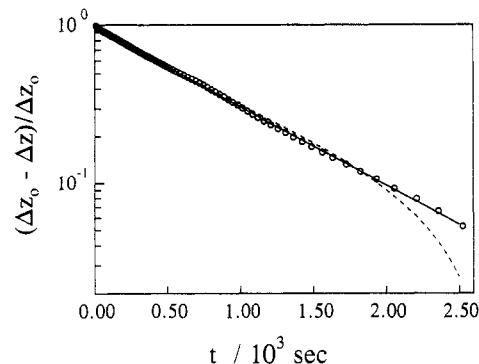


Figure 5.

thickness can be considered as infinite in practice. A three-dimensional problem is reduced into a one-dimensional one. Second, the film is so thin that we are able to assume that solvent can penetrate the thin gel film instantly. The difference between the surface and center in a thin gel film is relatively less than the one in a sample with macroscopic size. Third, the total experimental duration is considerably short, i.e., minutes instead of hours or even days, in comparison with the time reported in literatures,⁸⁻¹⁰ so that the swelling equilibrium can be reached in a reasonable time scale and the experimental conditions, such as temperature, can be better controlled.

According to eq 4, we are able to experimentally determine B_1 and τ_1 from the linear extrapolation of the long-time portion of $\ln[(W_\infty - W)/W_\infty]$ versus time. In our case, the solvent uptake (W) at time t is proportional to Δz , so that $\ln[(W_\infty - W)/W_\infty]$ can be replaced by $\ln[(\Delta z_0 - \Delta z)/\Delta z_0]$, i.e.

$$\ln\left(\frac{\Delta z_0 - \Delta z}{\Delta z_0}\right) = \sum_{n=1}^{\infty} B_n \exp(-t/\tau_n) \quad (10)$$

where Δz_0 is the film thickness increment at the final swelling equilibrium. Figure 5 shows a typical plot of $\ln[(\Delta z_0 - \Delta z)/\Delta z_0]$ versus t , where "o" are experimental data points. It can be seen that the data points have nearly fallen into a straight line except those very initial data points, which means that τ_1 is dominate and B_1 is close to 1. In Figure 5, for those data points of $>100 \text{ s}$, the continuous line represents a least-square fitting based on eq 4; and the broken line, a least-square fitting based on eq 1 where W and W_∞ have been replaced by Δz and Δz_0 , respectively. It is obvious that eq 4 describes the experimental data better. On the basis of Figure 5 one can see definite difference between the prediction of eqs 1 and 4 only at large time behavior. At short time swelling no difference can be established. All of the swelling kinetic data obtained in this work with different gelatin concen-

Table 1. Summary of B_1 , τ_1 , R , and D_c of Thin Gelatin Gel Film at Different Initial Gelatin Concentrations and Different Swelling Temperatures^a

C (W/W)	T (°C)	B_1	τ_1 (10^2 s)	R	D_c (10^{-7} cm ² /s)
10.0%	25	0.94	6.6	0.68	2.6
	29	0.96	8.3	0.70	2.1
	33	0.97	9.9	0.72	2.7
15.0%	25	0.94	6.0	0.68	2.5
	29	0.94	7.6	0.68	2.0
	34	0.96	8.7	0.70	2.2
20.0%	25	0.93	5.5	0.67	2.2
	29	0.95	6.9	0.69	2.6
	34	0.95	7.6	0.69	2.3

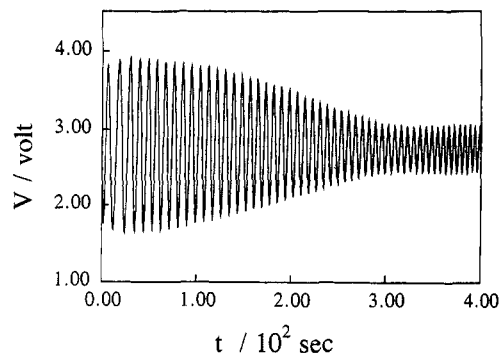
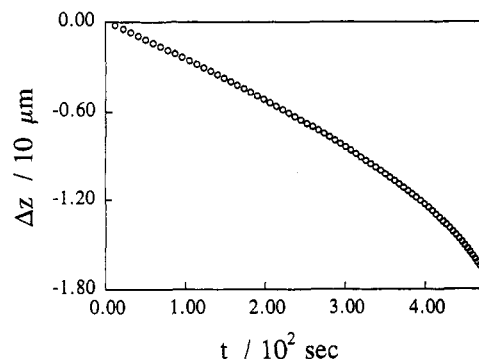
^a The relative errors are in the following: C , $\pm 2\%$; T , ± 0.2 °C; B_1 , $\pm 2\%$; τ_1 , $\pm 5\%$; R , $\pm 2\%$; and D_c , $\pm 15\%$.

trations and at different swelling temperatures can be better fitted by eq 4, which suggests that the swelling of thin gelatin gel film follows a first-order kinetics, not a second-order one, or in other words, the swelling behavior of thin gelatin gel film is similar to that of other types of polymer gels, such as polyacrylamide and poly(vinyl acetate) gels.⁸⁻¹⁰

This apparent difference between the present observed first-order kinetics and the past observed second-order kinetics might be due to the following two facts: First, the gelatin gel film is so thin that water can penetrate it in a very short time (~ 10 s). After that, the internal part of the gel fully contacts or interacts with water. Therefore, for $t > 100$ s, there should exist no such internal specific boundary areas which encloses those sites of the polymer network that have not interacted with water as suggested in ref 8. Thus, the swelling rate of thin gelatin gel film should be only proportional to the relative or fractional amount of swelling capacity still available at time t , i.e., following a first-order kinetics similar as in eq 5. Second, it takes so long for a macroscopic size gel to swell and reach its final and true swelling equilibrium state, especially near the end, the swelling becomes so slow that it is difficult to judge whether the equilibrium has been reached or not within a reasonable time scale. It can be seen in Figure 5 that if the measurement was stopped at $t = \sim 1800$ s, it would not be easy for us to tell the difference between the two lines, i.e., we cannot distinguish the first-order kinetics from the second-order one within the experimental uncertainties.

Experimentally, we found that the gel thickness, in the range of 15–90 μm , has no observable effect or influence on the order of swelling kinetics. Therefore, for the experimental convenience, we used the 60- μm gelatin gel films in the present work. The values of B_1 and τ_1 of thin gelatin gel films with different initial gelatin concentrations and at different gelling and swelling temperatures have been obtained from the least-square fitting of the kinetic data on the base of eq 4. The results are summarized in Table 1. All data listed in Table 1 are the average values from at least five repeated measurements. The $\pm 5\%$ relative error in τ_1 is mainly from the reproducibility of the repeated measurements, not from the least-square fitting. The larger 15% relative error in D_c is related to the uncertainty in the final equilibrium disk thickness, z_∞ , in eq 7.

Table 1 shows that B_1 (~ 0.95) is not strongly dependent on either the gelatin concentration or the swelling temperature and so does R . However, the obtained value of $R \sim 0.69$ for gelatin is significantly larger than that of ~ 0.3 – 0.4 obtained for other gels.^{8,10} This difference might be due to the difference between gelatin gel and those chemical gels since gelatin gel is formed by a renatural-

**Figure 6.****Figure 7.**

ization ("crystallization") process so that the expected cross-linking density is much higher, which leads to a higher shear modulus (G), i.e., a higher value of R . This difference might also be due to that gelatin has charges, and polyelectrolyte effects have not been considered in eq 4. Another reason can be that eq 4 was derived for chemically cross-linked networks. In this study a physical gel was considered. Table 1 also shows that τ_1 increases as temperature, but decreases as gelatin concentration, which is understandable since (i) at higher temperature the gel will be able to swell more and takes more time to reach its equilibrium state and (ii) the cross-linking density increases as gelatin concentration so that the gel will swell less and take less time to reach its fully swollen state. In Table 1, D_c is in the range of $\sim (2.0\text{--}2.7) \times 10^{-7}$ cm²/s which is in the same order as those listed in literatures.^{8,7,16}

Figure 6 shows one part of typical observed signal in drying process. It can be seen in Figure 6 that the time interval between two near maximums or minimums decreases as time, which is opposite to that in the swelling process. This can be more clearly seen in Figure 7 where we have transferred the signal in Figure 6 into the film thickness change (Δz) versus time (t). At the initial stage, Δz decreases almost linearly as t increases. Then, Δz decreases faster and faster until the gelatin gel film is completely dried out. At first, this really surprised us since according to eq 3 the decreasing rate of Δz should slow down and approach zero as time increases. We repeated the drying experiments with different initial gelatin concentrations and at different temperatures. This drying-rate-increasing process is confirmed by all experimental results. This obvious deviation from eq 3 might come from the following two facts:

First, in the drying process, the surrounding is dry air which is quite different from solvent (water) in the shrinking process. In the shrinking process, due to the effect of osmotic pressure, the diffusion of solvent from the inside of gel to outside of gel should become more and more difficult as more and more water is "squeezed" out from the gel in the shrinking process, i.e., the decreasing

rate in the gel thickness should decrease. But, in the drying process, the chemical potential of solvent inside the gel is always larger than that outside of the gel because there is no solvent outside. Therefore, there is no extra hindering force outside to prevent the escape of solvent from the gel. Second, the gelatin gel is formed by the physical cross-linking, i.e. by the triple-stranded helix ("crystallization"). In the drying or shrinking process, the degree or density of cross-linking inside a gelatin gel is not fixed as that inside a chemically cross-linked gel. During the drying process, as solvent escapes from the gel, the gel thickness decreases, i.e., the average interspace between gelatin molecules decreases, so that gelatin molecules have more tendency or chance to form new cross-linking points, or say, to form more triple-stranded helices. This increment in the cross-linking density in turn further reduces the average interspace between gelatin chains, i.e., the gel thickness.

After combining the above two facts together, it is not very difficult for us to imagine that as time increases the drying rate increases, not decreases, as expected in a shrinking process. However, up to now, we are still not able to formulate a quantitative kinetic theory to describe this complicated drying process. In general, we have observed that the drying speed increases with temperature and decreases as the initial gelatin concentration increases. Qualitatively, this can be explained in the following: on the one hand, water molecules inside the gel have more energy to escape from the gel at the higher drying temperature, and on the other hand, the amount of the triple-stranded helices formed at higher temperature is relatively lower, so that the cross-linking density is lower, which enables the escape of water from the gel more easily. As for the effect of the initial gelatin concentration, it can also be explained in terms of the amount of the triple-stranded helices, or the cross-linking density, since it increases with the concentration.

Conclusions

We have shown that the swelling of thin gelatin gel film can be better described by the first-order kinetics predicted by Li and Tanaka. The observed second-order swelling kinetics for the gelatin samples in the past might be due to the relatively larger sample size. We also shown that

the estimated ratio of the shear modulus over the longitudinal modulus for thin gelatin gel film is relatively larger than that for those loosely cross-linked chemical gels, such as polyacrylamide and poly(vinyl acetate), which might be due to the difference in both the cross-linking density and the cross-linking nature. The estimated values of the cooperative diffusion coefficient ($D_c \approx 2.5 \times 10^{-7} \text{ cm}^2/\text{s}$) are comparable to those listed in literatures. We also observed that the drying rate of the thin gelatin gel films in dry air increases with time instead of a slow-down process expected in the gel-shrinking process. This unexpected drying kinetics might be attributed to the difference between the drying process and the shrinking process and to the nature of gelatin gel formation. The successful applications of *in situ* interferometry in the studies of gelatin gels has shown that this *in situ* method is ready to be used to study the swelling or shrinking behaviors of other types of polymer networks or gels.

Acknowledgment. We thank Miss Lun Chui Ying for her participating in part of the reported experimental works. We also gratefully acknowledge the financial support of this work by the RGC (the Research Grants Council of Hong Kong Government) Earmarked Grant 1993/94 (CUHK 79/93E, 221600140).

References and Notes

- (1) Flory, P. J. *Principle of Polymer Chemistry*; Cornell University Press: Ithaca, NY, 1953.
- (2) Dusek, K.; Prins, W. J. *Adv. Polym. Sci.* **1969**, *6*, 1.
- (3) Tobolsky, A. V.; Goebel, J. C. *Macromolecules* **1970**, *3*, 556.
- (4) Amiya, T.; Tanaka, T. *Macromolecules* **1987**, *20*, 1162.
- (5) Schild, H. G. *Prog. Polym. Sci.* **1992**, *17*, 163 and references therein.
- (6) Tanaka, T.; Fillmore, D. J. *J. Chem. Phys.* **1979**, *70* (3), 1214.
- (7) Peters, A.; Candau, S. J. *Macromolecules* **1988**, *21*, 2278.
- (8) Li, Y.; Tanaka, T. *J. Chem. Phys.* **1990**, *92* (2), 1365.
- (9) Schott, H. J. *Macromol. Sci., Phys.* **1992**, *B31* (1), 1.
- (10) Zrinyi, M.; Rosta, J.; Horkay, F. *Macromolecules* **1993**, *26*, 3097.
- (11) Ward, A. G.; Courts, A. *The Science and Technology of Gelatin*; Academic Press: London, 1977.
- (12) Veis, A. *The Macromolecular Chemistry of Gelatin*; Academic Press: London, 1964.
- (13) Ofner, C. M., III; Schott, H. J. *Pharm. Sci.* **1987**, *76*, 715.
- (14) Robinson, I. D. *Photograph. Sci. Eng.* **1964**, *8*, 220.
- (15) de Bore, J.; Visser, R. J.; Melis, G. P. *Polymer* **1992**, *33* (6), 1123.
- (16) Tanaka, T.; Hocker, L.; Benedek, G. *J. Chem. Phys.* **1973**, *59*, 5151.